Wood Material Science & Engineering, 2016
Vol. 11, No. 4, 228–238, http://dx.doi.org/10.1080/17480272.2014.973443

Taylor & Francis
Taylor & Francis Group

ORIGINAL ARTICLE

Moisture storage and transport properties of preservative treated and untreated southern pine wood

SAMUEL L. ZELINKA[1], SAMUEL V. GLASS[1], CHARLES R. BOARDMAN[1], & DOMINIQUE DEROME[2]

[1]*Building and Fire Sciences, US Forest Service, Forest Products Laboratory, Madison, WI, USA,* [2]*Laboratory of Building Science and Technology, EMPA, Duebendorf, Switzerland*

Abstract
Moisture storage and transport properties of southern pine (*Pinus spp.*) wood were measured for implementation into hygrothermal models. Specimens were untreated or pressure-treated with alkaline copper quaternary (ACQ) preservative. Moisture storage was characterized with sorption isotherms in the hygroscopic region (high capillary pressures) and documented with mercury intrusion porosimetry in the overhygroscopic region (low capillary pressures). The data were then combined into a single moisture retention curve as a function of capillary pressure. Moisture transport was evaluated from steady-state water vapor transmission and dynamic capillary water absorption experiments. These data were used to calculate the moisture permeability over the entire range of capillary pressures using the diffusivity approach of Carmeliet *et al.* Moisture storage and transport properties were similar for the untreated and ACQ-treated southern pine, except for the permeability of the treated wood which was lower in the radial direction. The data presented here can be used to improve the accuracy of hygrothermal and combined hygrothermal–corrosion modeling simulations.

Keywords: *Southern pine, water vapor transmission, capillary absorption, sorption isotherm, mercury intrusion porosimetry, hygrothermal modeling*

Introduction

Recently, a combined hygrothermal and corrosion model was developed for fasteners in treated wood (Zelinka *et al.* 2011). The model uses climatic data and material hygrothermal properties as inputs and calculates the temperature, wood moisture content, and depth of corrosion penetration along the length of the fastener. The motivation was to examine how recent changes in wood preservative regulation (Lebow 2004) may affect the service life of fasteners, as newer waterborne wood preservatives, such as copper azole, alkaline copper quaternary (ACQ), and so-called "micronized" formulations, have been shown to be more corrosive than the chromated copper arsenate (CCA) treatment that they have replaced (Zelinka and Stone 2011, Zelinka and Rammer 2012). The model used an existing, two-dimensional, finite element hygrothermal model developed by Janssen *et al.* (2007) (HAMFEM) to calculate the wood moisture content. The hourly averaged wood moisture content was then combined with a corrosion model where the metal corrosion rate depended on the local wood moisture content. The simulations were run with hygrothermal properties of European spruce (Zillig 2009) and the corrosion model was based upon empirical corrosion data collected from both electrochemical (Dennis *et al.* 1995, Short and Dennis 1997) and gravimetric corrosion rates measured in wood treated with ACQ (Zelinka *et al.* 2008).

The development of the combined hygrothermal–corrosion model has spurred additional research to understand how well the model predictions compare with field corrosion data. Further research has been conducted to better understand the relationship between the corrosion rate of steel and galvanized steel as a function of wood moisture content

Correspondence: Samuel L. Zelinka, Durability and Wood Protection Research, US Forest Service, Forest Products Laboratory, Madison, WI, USA. Tel: +1 608 231 9277. Fax: +1 608 231 9303. E-mail: szelinka@fs.fed.us

(*Received 12 September 2014; revised 1 October 2014; accepted 2 October 2014*)

(Zelinka *et al.* 2014). There is a similar need to characterize the moisture retention and transport properties of wood treated with waterborne wood preservatives to improve the accuracy of combined hygrothermal and corrosion modeling.

Over 95% of the preservative-treated wood in the USA is from the southern pine (*Pinus spp.*) species group (Vlosky 2009). The southern pine species group consists principally of longleaf pine (*Pinus palustris*), loblolly pine (*Pinus taeda*), shortleaf pine (*Pinus echinata*), and slash pine (*Pinus elliottii*); these species cannot be distinguished by wood anatomy or other physical or chemical characteristics (Anon. 1936). Southern pine is frequently used with preservative treatments because it has a large percentage of sapwood, which easily accepts preservative treatment when pressure-treated (Lebow 2010).

Wood anatomical characteristics can explain why southern pine sapwood can be easily treated. Softwoods are mainly composed of tracheids, which are hollow cylinders roughly 3 mm long and 30–40 μm in diameter (Wiedenhoeft 2010). The tracheids are connected to adjacent tracheids through check valve like structures called bordered pits, whose purpose is to contain embolisms in the living tree (Zwieniecki and Holbrook 2000, Holbrook *et al.* 2002). The bordered pits irreversibly aspirate during heartwood formation. Because southern pine has a large percentage of sapwood, the bordered pits are not irreversibly aspirated, and the aqueous preservative treatment solution can more easily travel between adjacent cells. One could therefore expect that liquid water transport in southern pine would be much more rapid than in a species with a high percentage of heartwood, such as the European spruce used in the initial combined hygrothermal–corrosion modeling (Zelinka *et al.* 2011).

Hygric property data for southern pine in the literature are abundant for the sorption isotherm but scarce for moisture retention in the overhygroscopic range as well as for moisture transfer. Glass *et al.* (2014) compared adsorption and desorption isotherms for southern pine from various sources. Measurements of moisture retention in the overhygroscopic range have been made by Zhang and Peralta (1999) and by Kumaran *et al.* (2002), though the latter acknowledge that their data are far removed from equilibrium values. Transverse moisture diffusion in the hygroscopic range has been measured by Kumaran *et al.* (2002) using a steady-state method and by Neimsuwan *et al.* (2008) using a dynamic method. Kumaran *et al.* (2002) have also measured transverse and longitudinal liquid water absorption. Given the limited data available, characterizing moisture retention and moisture transfer in all three principle directions in southern pine was deemed worthwhile to provide a consistent data-set for hygrothermal modeling.

The preservative treatment process may also affect wood anatomical features that control moisture transport properties. During treatment with wood preservatives, the wood is immersed in liquid and then exposed to through vacuum and pressure cycles. This treatment process may tear the wood cell pits, and even walls, changing the pore size distribution, which affects both the moisture storage and transport properties of the wood. Furthermore, the treatment chemicals may affect the hygroscopicity of the wood. There has been little work on whether preservative treatments affect the moisture retention and moisture transport properties in wood. The only property that has been characterized in the literature is the sorption isotherm, which has been characterized for wood treated with CCA, copper ethanolamine, borates, and ACQ (Dulat 1980, Shupe *et al.* 2001, Cao and Kamdem 2004, Zelinka and Glass 2010).

This paper presents hygric properties of ACQ-treated and untreated southern pine wood that can be implemented in hygrothermal models. Moisture storage is characterized by the sorption isotherm in the hygroscopic region and by mercury intrusion porosimetry (MIP) in the overhygroscopic region. Moisture transport is characterized by the water vapor transmission and capillary absorption tests; the data are treated with the diffusivity approach of Carmeliet *et al.* (2007) to describe moisture transport over the full range of moisture contents. The data are the first on the moisture storage and transport of preservative-treated wood and will be used to validate a field test of the combined hygrothermal–corrosion model.

Materials and methods

Materials

All material was cut from the same parent board, which was 250 mm by 250 mm by 7 m long (Figure 1). The board was southern pine (*Pinus sp.*), harvested from central Florida. Although the exact species could not be determined, it came from a plantation where 90% of the trees were slash pine (*P. elliottii*). In transit to the laboratory, the board was partially colonized by a blue stain fungus. Blue stain fungi and, more generally, sap-stain fungi do not affect the strength properties but may affect the interaction of water with wood (Findlay and Pettifor 1939, Schirp *et al.* 2003, Fojutowski 2004). While this colonization may change the hygrothermal properties from published values, blue stain fungi are commonly found on construction lumber, and therefore measuring wood with blue

Figure 1. Southern pine beam as delivered to Forest Products Laboratory. The cardboard pinned to the end grain shows the orientation of samples cut along the true radial direction.

stain, may provide a better representation of what is found in the real world.

Samples were cut from the parent beam along the three true anatomical directions for the moisture transport tests. Specimen dimensions are given below for each type of measurement. Half of the specimens were treated with alkaline copper quaternary type "D" with a carbonate formulation (ACQ-D). Specimens were treated to a retention of 4 kg m^{-3} of preservative, which corresponds with AWPA use category 3 for above ground use (Anon. 2007). Half of the specimens were treated by submerging the wood in an ACQ-D solution and pulling a vacuum (3.7 kPa) for 30 minutes.

Methods

Density and saturated moisture content. The density and saturated moisture content of the wood were measured on 20 replicates on 25 mm cubes cut from various positions along the parent board. The cubes were submerged underwater and a vacuum (3.7 kPa) was pulled for 30 minutes. The specimens were kept underwater overnight. Upon removal from the water, the specimen mass and dimensions were measured. The specimens were then oven-dried and again mass and dimensions were measured.

The (oven-dry) density was taken as m_{od}/V_{od} where m is the mass (kg), V is the volume (m^3), and the subscript "$_{od}$" represents oven-dried. The maximum moisture content was taken as $(m_{sat} - m_{od})/m_{od}$ in units of kilogram per kilogram (or expressed as %MC) or equivalently $(m_{sat} - m_{od})/V_{od}$ in units of kilogram per cubic meter where m_{sat} is the mass of the water saturated specimen.

Moisture retention curve. The moisture retention curve in the hygroscopic region (0–95% RH) was taken from the sorption isotherm, which was collected with an IGASorp gravimetric vapor sorption analyzer (Hiden Isochema, Warrington, UK). The isotherm was collected at 25°C. Relative humidity was controlled with mass flow controllers by mixing saturated and dry nitrogen gas at constant flow over the specimen. The adsorption isotherm was collected in increments of 5% RH starting at 5% and ending at 95%; prior to the first step, the specimen was exposed to dry nitrogen (~0% RH) for 2 hours at 40°C. The desorption isotherm was collected immediately after the adsorption isotherm, with the first step being 90% RH decreasing to 5% RH in increments of 5%. The oven-dry mass was measured by heating the sample to 105°C under dry nitrogen to constant mass.

The overhygroscopic region was characterized with MIP, which characterizes the volume of pores across a range of diameters. The measurements were taken with a Pascal 440 porosimeter (Thermo Scientific, Waltham, MA, USA) at 25°C from 0.12 MPa to 200 MPa. Prior to MIP measurements, the wood was cut into 300 μm sections with a sliding microtome, as suggested by Trenard (1980), so that the mercury could infiltrate all lumina.

Moisture transport properties

Water vapor diffusion (cup test)

Moisture transfer in the hygroscopic region was characterized using a cup test, where the wood specimen was sealed to the lid of a cup containing a saturated salt solution to maintain a constant relative humidity. The cup assembly was placed in a chamber at 23°C with a controlled relative humidity. The water vapor transport experiments were run on samples nominally 13 mm thick; the length and width of the specimen depended on how large of a sample could be cut with the curvature of the growth rings. The radial specimens were 56 mm (T) by 132

mm (L), and the longitudinal and tangential specimens were 81 (R) by 132 mm (L). The edges of these samples were sealed with hot paraffin wax.

Three different conditions were tested: 11% RH/50% RH, 94% RH/50% RH, and 94% RH/80% RH (inside/outside) resulting in average relative humidities of 30.5, 72, and 88%, respectively. The relative humidity in the cup was fixed by saturated salt solutions; either LiCl-11% RH or KNO_3-94% RH. The temperature and relative humidity outside of the cup were controlled by placing the cup inside of an environmental chamber capable of maintaining ±0.1% RH and ±0.1°C. The cup was placed on a balance attached to a data acquisition system so that the mass loss (gain) could be continuously recorded. The slope (mass vs. time) changed considerably during the first 400 hours of the test caused by moisture sorption/desorption in the material. After 400 hours, the slope remained relatively constant. The vapor diffusion resistance factor, μ, was calculated from the average slope of the mass vs. time curve, $\dot{m}$ (kg s^{-1}) between 400 and 500 hours of the test through

$$\mu = \frac{\delta_a A(\Delta p_v)}{\dot{m} d},$$

where A is the area of the sample (m^2), d is the specimen thickness (m), Δp_v is the difference in vapor pressure across the specimen (Pa), and δ_a is the water vapor permeability of still air at 23°C (2.05×10^{-10} kg m^{-1} s^{-1} Pa^{-1}). Raw data were corrected with an edge correction factor to account for wax masking the specimen edges and correction factors for the resistance of still air inside of the cup and the interior and exterior surface resistances. Replicates were run in parallel and used manual measurements; the duration of the test was based upon our knowledge of the time taken to reach steady state from the continuous data acquisition system.

Liquid water uptake

The liquid water diffusivity was characterized from a capillary uptake test where a 50 mm cube with four sides sealed was brought into contact with liquid water and the mass of the block was measured as a function of time. The experiments were conducted in a unique apparatus where the block was suspended from a load cell so that data could be collected continuously without removing the specimen from the water (Figure 2). The sides were sealed with neoprene paint which we found to give the best edge sealing in preliminary tests. During testing, a small plate with a bulls-eye level in the middle of it was placed on top of the specimen to make sure that the specimen was parallel to the water front and the plate also prevented drying of the specimen from the top while allowing the gas pressure within the sample to remain at one atmosphere.

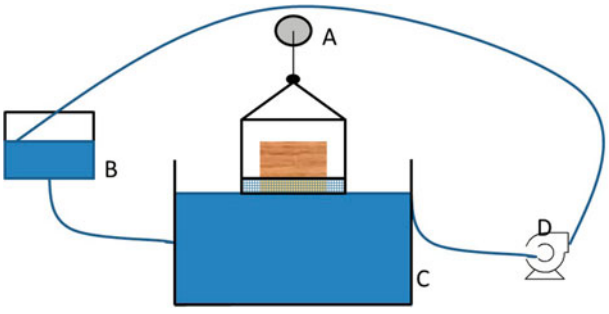

Figure 2. Schematic of the capillary absorption apparatus, where the sample was suspended from a load cell (A). Water level was maintained by a secondary reservoir (B), a weir notched into the primary reservoir (C), and a pump (D).

Traditionally the capillary absorption data are treated by plotting the mass uptake as a function of the square root of time. This plot yields the capillary absorption coefficient "A_{cap}," which is the initial slope of the curve, and the capillary moisture content "w_{cap}," which is the moisture content at which the curve deviates from linearity and is found by the intersection of the initial slope with the slope taken at higher moisture contents above the capillary limit. This data treatment presupposes that the data exhibit bilinear behavior or at least an initial linear region. We found that in all cases, there was no distinct initial linear region followed by a plateau; rather, the slope appeared to be continuously decreasing, and even after long times the samples continued to gain mass (e.g. Figure 3). Such

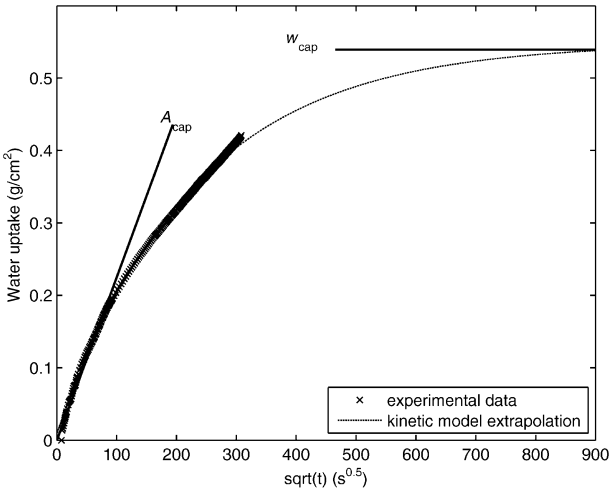

Figure 3. Illustration of how the capillary absorption data were processed. A_{cap} was calculated from the average slope over the first hour of the test. w_{cap} was found by extrapolating the data with an asymptotic function and dividing by the sample thickness.

behavior, attributed to swelling, was also documented for spruce by Zillig (2009). To process these data for hygrothermal modeling, we took the capillary sorption coefficient as the average slope over the first hour of the test; given our data acquisition rate, this represented an average over 450 points. This criterion was chosen as hygrothermal models often use hourly climatic data as inputs. Although the data did not exhibit a clear discontinuity suggesting the capillary limit had been reached, the slope of the curve was continuously decreasing and it appeared that it would eventually reach an asymptote. To estimate the capillary moisture content, we fit the data to a simple first-order kinetic model

$$\frac{dm(t)}{dt} = -k \cdot m(t),$$

where k is the time constant of the step change. This model is frequently used to calculate the moisture content arising from a step change in relative humidity. Figure 3 illustrates our manner of data reduction with A_{cap} and w_{cap} (multiplied by the sample thickness) highlighted on the graph.

Results

Density and saturated moisture content

The average density (dry weight and dry volume) of the 16 cubes that was 445 (±1) kg m^{-3} (all error bars are reported as standard error). Often the basic specific gravity, which is a ratio of the oven-dry weight divided by the green (saturated) volume divided by the density of water (1000 kg m^{-3}), is tabulated for wood. The basic specific gravity was found to be 0.401 ± 0.001.

There was more variation in the saturated moisture content of the specimens. The average saturated moisture content was 725 (±4) kg m^{-3} or equivalently 163% MC (±2%), and ranged from a low of 695 kg m^{-3} (141% MC) to a high of 750 kg m^{-3} (176% MC). Qualitatively, the specimens that were outwardly exhibiting signs of colonization by the blue stain fungus had a higher saturated moisture content.

Moisture retention curve

The sorption isotherms for treated and untreated southern pine are shown in Figure 4 for both adsorption and desorption. Specimens were run in triplicate through one cycle of adsorption and desorption; replicate specimens were identical. Comparing the treated and untreated pine, the adsorption curves were very similar and the desorption isotherm was slightly lower for the ACQ-treated

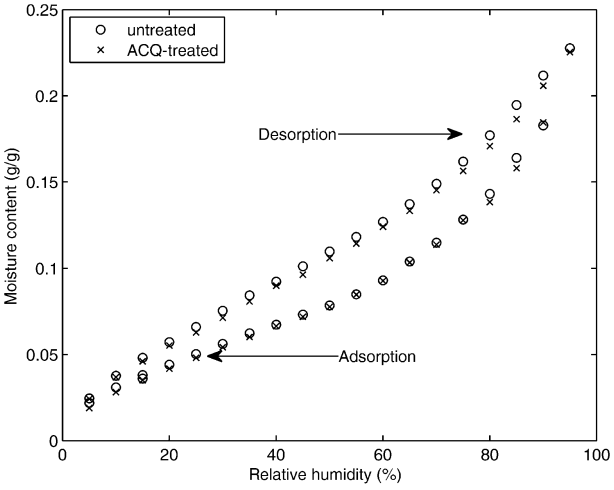

Figure 4. Water vapor sorption isotherms for ACQ-treated and untreated wood taken at 25°C.

data. The desorption branch of the sorption isotherms was combined with the mercury intrusion data to form the entire moisture retention curve.

Figure 5 shows a mercury volume/mercury pressure curve collected for the treated and untreated southern pine. Replicates curve for both the treated and untreated pine were virtually indistinguishable from these curves. Therefore, the data in Figure 5 were used to calculate the overhygroscopic region of the moisture retention curve.

To create the moisture retention curve for the overhygroscopic region, the mercury pressure (P_{Hg}) was converted to the capillary pressure (p_c) by

$$p_c = -P_{Hg}\left(\frac{\sigma_{H_2O}\cos\theta_{H_2O}}{\sigma_{Hg}\cos\theta_{Hg}}\right),$$

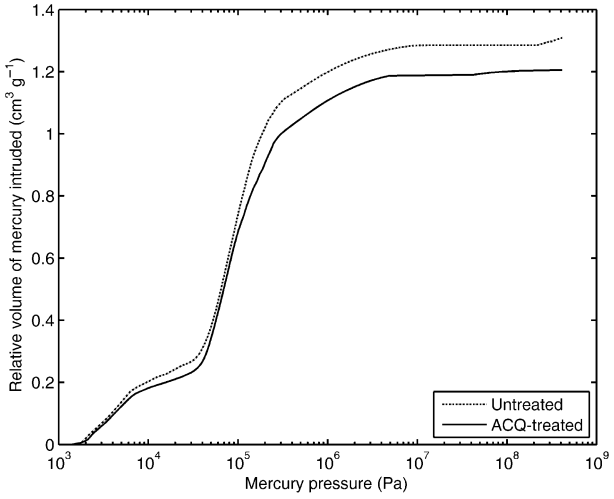

Figure 5. Mercury pressure/volume curve used to generate the moisture retention curve.

where σ is the surface tension (N m^{-1}) and θ is the contact angle. Water was assumed to be perfectly wetting ($\theta = 0$) and the commonly assumed value of 130° was used for the contact angle of mercury. Capillary pressure physically represents the difference between the gas pressure and liquid pressure and is a way to express the chemical potential of water, μ_{H_2O}, or water activity, a_w (which is equivalent to the fractional relative humidity for water vapor). Mathematically, the capillary pressure can be represented by

$$p_c = \begin{cases} P_g - P_l \\ -\rho_l R_v T \ln a_w \\ -\mu_{H_2O}/V_m \end{cases},$$

where P_g and P_l are the gas and liquid pressures, respectively, ρ_l is the density of liquid water, R_v is the specific gas constant for water vapor, and V_m is the molar volume of liquid water.

The mercury volume was converted to moisture content in kilogram per cubic metre by

$$w = w_{sat} - \left[(\nu - \nu_o)\rho_{wood}^{dry}\right]\rho_{H_2O},$$

where v is the specific volume of mercury filled (m^3 of mercury per kg of dry wood) at pressure P_{Hg} and ν_o is the specific volume of mercury intruded at the lowest P_{Hg}.

Figure 6 shows the combined moisture retention curve for the untreated and treated pine. The capillary moisture content, w_{cap}, is illustrated on the curve; this is the maximum moisture content that the wood will see under in-service conditions. Since the untreated and ACQ-treated curves were virtually identical until w_{cap}, the same moisture retention curve could be used for both the ACQ and untreated wood. The moisture retention curve used in modeling was found by fitting the data in Figure 6 (truncated at w_{cap}) with a two-part van Genuchen equation (Durner 1994, Carmeliet and Roels 2002; illustrated as a solid line) of the form

$$w = w_{cap}\sum_{i=1}^{2} l_i\left[1 + (a_i p_c)^{ni}\right]^{-mi},$$

where *l, a, n, and m* are fit parameters. The parameters from the curve fit are given in Table I. The data used for modeling are shown in the pore systems highlighted in Figure 7. For comparison, we include the data of Zhang and Peralta (1999).

Table I. Fit parameters of the moisture retention curve used in modeling. The parameter w_{cap} was 454 kg m^{-3}.

	Pore system	
	1	2
l	0.730	0.2670
a	$6.66 \times 10^{-0.5}$	$3.25 \times 10^{-0.8}$
n	3.451	1.77
m	−0.710	−0.436

Vapor diffusion

The vapor diffusion resistance factor was collected for the three anatomical directions at three different relative humidity boundary conditions for both the

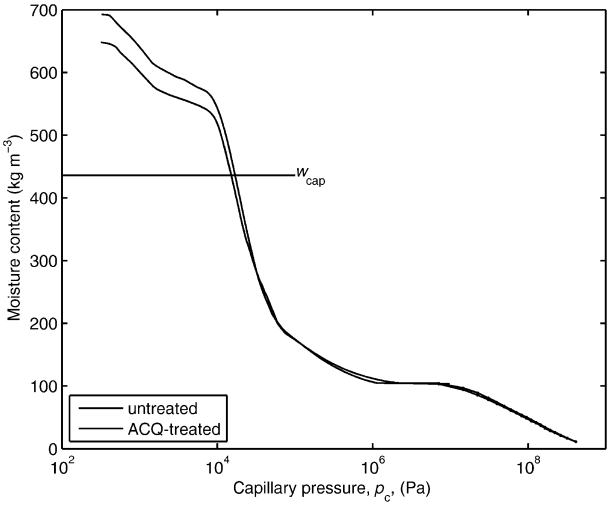

Figure 6. The moisture content as a function of capillary pressure for the untreated and treated wood; note that the moisture content is the same for each until w_{cap} and therefore the moisture storage of the untreated and treated wood can be handled by the same function for modeling purposes.

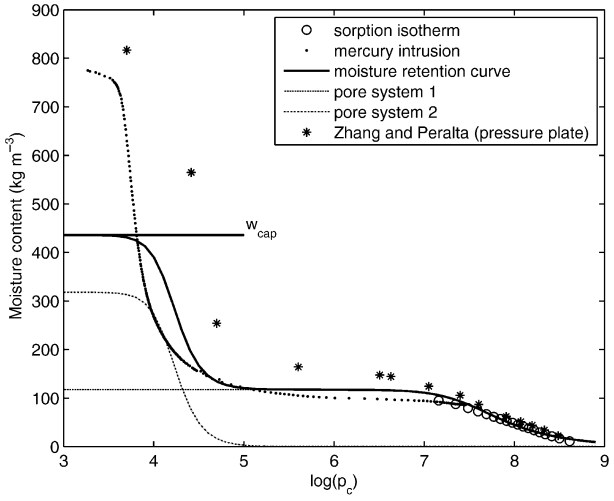

Figure 7. Moisture retention curve (solid line) used for modeling pine found by fitting the combined desorption data and mercury intrusion data with a van Genuchen equation. The different pore systems from the van Genuchen equation are highlighted. The data of Zhang and Peralta (1999) are included for comparison.

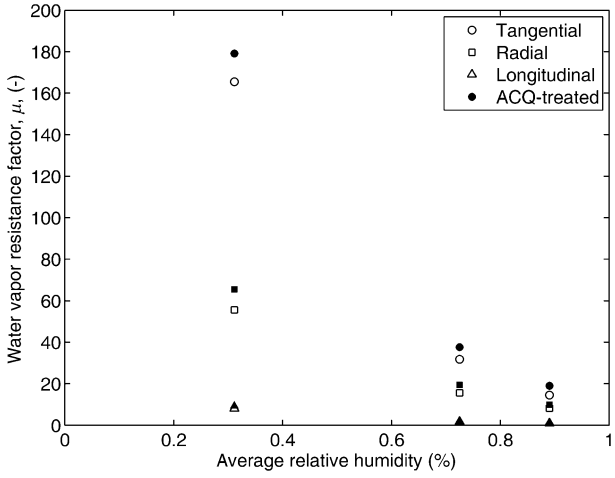

Figure 8. Vapor diffusion resistance factors for the tangential, radial, and longitudinal directions. Filled symbols represent the ACQ-treated samples of the similar orientation (i.e. a filled triangle represents ACQ-treated wood measured in the longitudinal direction).

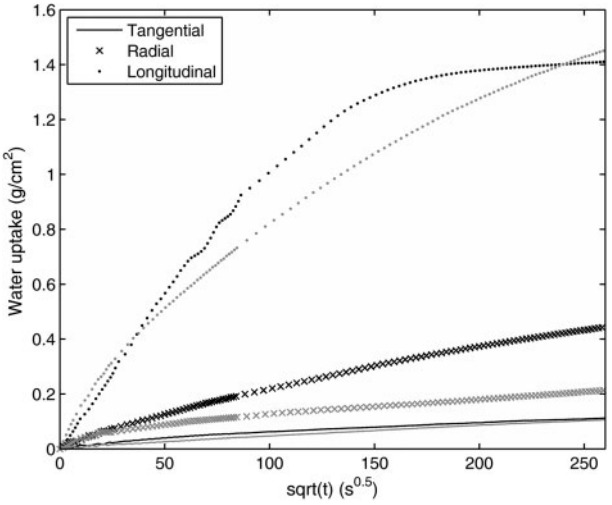

Figure 9. Example capillary absorption curves for the three anatomical directions in untreated wood (black) and ACQ-treated wood (gray). For the radial and longitudinal directions, only 1 out of every 15 data points are plotted so that the symbols can be differentiated on the graph. Note that absorption was much lower in the treated wood in the radial direction.

treated and untreated southern pine, with three replicates for each parameter. The average vapor diffusion resistance factors for each anatomical direction for treated and untreated wood are plotted in Figure 8 and listed in Table II with the standard error. The data show treated wood has a slightly higher vapor resistance factor in each anatomical direction. However, because of the small sample size, this difference is not statistically significant.

For both the treated and untreated wood, in the longitudinal direction and highest relative humidity tested, μ was very close to, or slightly less than unity, which represents a physical lower boundary. Since the permeability was very high in this direction, the uncertainties from the measurement technique from the masked sample edge and still air layer have a large effect on the measured values. We took $\mu = 1$ when calculating the permeability in the longitudinal direction at the highest relative humidity; however, the values reported in Table II should be used with caution.

Table II. Water vapor diffusion resistance factor as a function of relative humidity.

		μ(–)	
	Relative humidity(–)	Untreated wood	ACQ-treated wood
Tangential	0.31	166 (5)	179 (42)
	0.725	32 (0.1)	38 (6)
	0.89	15 (1)	19 (4)
Radial	0.31	56 (6)	66 (5)
	0.725	16 (1)	19 (3)
	0.89	8 (2)	10 (6)
Longitudinal	0.31	8 (4)	9 (0.3)
	0.725	2 (0.3)	2 (0.3)
	0.89	1 (0.7)	1 (0.6)

The quantity in parentheses represents the standard error.

Capillary sorption

Example curves, taken from the three replicates of each factor, of the capillary absorption data for the three anatomical directions and two treatments are plotted in Figure 9. Although the data lack a clear linear region or plateau, the method of data reduction shown in Figure 3 allowed us to calculate A_{cap} and w_{cap}. In theory, the w_{cap} should not depend upon the anatomical direction and therefore a grand average was taken for the treated and untreated data and used for modeling. The resulting w_{cap} was found to be 454 kg m^{-3}. However, the w_{cap} data vary widely across the different anatomical directions. This is likely caused by the shape of the curve and the extrapolation, and suggests that the w_{cap} data should be used with caution. The capillary absorption coefficient (A_{cap}) calculated from the first hour of the test is listed in Table III with their standard errors. For the tangential and longitudinal directions, differences between the treated and untreated wood were minor and within the standard error of the measurements. However, for the radial direction, the capillary absorption coefficient of the ACQ-treated wood was half that of the untreated wood, and it appears that the treatment is affecting liquid water transport in the radial direction.

Table III. Capillary absorption coefficient, A_{cap}, determined from the average slope during the first hour of the capillary absorption test.

	A_{cap} (kg m^{-2} s$^{-0.5}$)	
	Untreated wood	ACQ-treated wood
Tangential	0.009 (0.002)	0.009 (0.002)
Radial	0.023 (0.003)	0.015 (0.004)
Longitudinal	0.087 (0.013)	0.087 (0.010)

The quantity in parentheses represents the standard error.

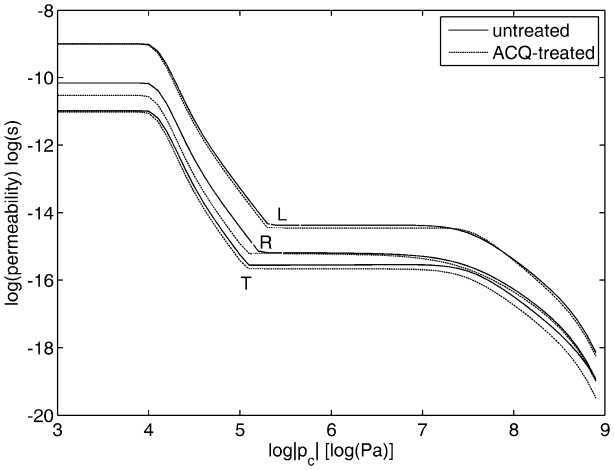

Figure 10. Permeability for untreated and ACQ-treated wood as a function of capillary pressure for the three anatomical directions of wood.

Moisture diffusivity

The hygrothermal data were implemented as a diffusivity using the approach of Carmeliet *et al.* (2007) where the moisture transport can be described by

$$\frac{\partial w}{\partial t} = \nabla D \nabla w,$$

where D is the moisture diffusivity. The diffusivity is calculated in two distinct regions by

$$\log D_1 = a + [\log D_o - a]\exp(-bw) + cw \ (\text{for} w < w_l)$$

where D_o is the diffusivity extrapolated to zero moisture content, and

$$\log D_2 = \frac{F}{\ln(10)}\left(\frac{w - w_{cap}}{w_{cap}}\right) + \log D_{w_{cap}} \ (\text{for} w \geq w_l).$$

We used a modified expression[1] for D_1 that has the same number of fitting parameters and a similar mathematical shape, but is simpler to fit

$$\log D_1 = aw^2 + bw + c \ (\text{for} w < w_l).$$

The diffusivity can be described by seven parameters: w_{cap}, the capillary moisture content; $D_{w_{cap}}$, the diffusivity at w_{cap}: F, the slope of the linear region: $_{wl}$, the limiting moisture content that represents the transition from D_1 to D_2; and fitting parameters a, b, and c. The diffusivity at w_{cap} can be determined by

$$D(w_{cap}) = f(F)\left(\frac{A_{cap}}{w_{cap}}\right)^2,$$

where

$$f(F) = \frac{F^2}{2F - 1 - e^F\left(F - 1 + \left(\frac{3}{2} - \frac{4}{\pi}\right)F^2\right)}.$$

The parameters a, b, and c were determined by fitting the three vapor diffusivities measured in the cup test. A_{cap} and w_{cap} were determined in the capillary sorption experiment. This leaves two unknowns, F and wl, for which we used values of 7.5 and 120 kg m^{-3}, respectively. Carmeliet *et al.* note that frequently F cannot be determined experimentally and, in these cases, a value of 7.5 is often assumed, as this is in the middle of the range of experimentally observed Fs (5–10) (Carmeliet *et al.* 2007). Other researchers who have applied the diffusivity model to wood have used a value of 7.5 as well (Zillig *et al.* 2006, Zelinka *et al.* 2010, 2011). The value of the limiting moisture content was chosen so that the function was smooth, and corresponded to a relative humidity of 99.9%.

The moisture permeability, K, ($K \equiv C \bullet D$), where C is the moisture capacity, that is the derivative of the moisture retention curve ($\partial w/\partial p_c$), is plotted as a function of capillary pressure for the different anatomical directions and treatments in Figure 10. As expected, the permeability was lowest along the tangential direction, higher in the radial direction (because of the ray cells), and highest in the longitudinal direction. For the longitudinal direction, the permeability was nearly identical for untreated and ACQ-treated wood. In the radial direction, the permeability at low capillary pressures (high moisture contents) was lower for the ACQ-treated wood than it was for the untreated wood.

Discussion

The goal of this work was to collect data on the hygric properties of untreated and ACQ-treated southern pine to improve the accuracy of hygrothermal models. It is worthwhile to compare the differences or lack of differences in the treated southern

pine. The ACQ treatment did not appreciably affect the moisture storage properties of the pine. Likewise, the permeability of the untreated and ACQ-treated southern pine was nearly identical for the tangential and longitudinal directions. These minor differences could likely be ignored for most modeling purposes. However, in the radial direction, the permeability of the ACQ-treated wood was much lower than the untreated wood.

It is interesting that preservative treatment only affects the permeability in the radial direction. While the water vapor transport was slightly lower for the treated wood in all directions (Figure 8), these small differences did not greatly affect the permeability (Figure 10). However, the liquid water uptake for the ACQ-treated wood was almost half as fast as the untreated in the radial direction, which caused the permeability be about an order of magnitude lower at low capillary pressures (high water activity). The fact that treatment only affects the radial properties suggests that the treatment, or the treatment processes, may affect the ray cells since these cells are responsible for the increase in permeability between the tangential and radial directions (Zillig 2009). It is possible that the treatment undergoes a different chemical reaction in the ray cells as opposed to the tracheids that then cause blockages to liquid water transport (i.e. pit aspiration).

Although there are few literature data for comparison, it is worthwhile to compare the current measurements to the range of previously published values. For the capillary absorption coefficient of untreated southern pine, Kumaran *et al.* (2002) observed a value of 0.0014 kg m^{-2} $s^{-0.5}$ but do not state whether the measurements were in the radial or tangential direction, and potentially the measurements could have been taken along a plane intermediate to the radial and tangential directions. Interestingly, our measured tangential (0.009) and radial (0.023) coefficients for untreated wood are 6 and 16 times larger, respectively. Our measured values are also larger than the value of 0.004 kg m^{-2} $s^{-0.5}$ in the IEA Annex 14 catalog of material properties for pine "perpendicular" to the fibers, although the exact species was not listed (Hens 1991). Our value in the longitudinal (0.087 kg m^{-2} $s^{-0.5}$) direction was also more than 5 times higher than the value listed IEA Annex 14 (0.163) (Hens 1991).

The moisture retention curve is similar to the one collected by Zhang and Peralta (1999) using the pressure plate technique. It should be noted that the density of their specimens was greater than ours; they found the basic specific gravity as 0.45 whereas our specimen had a basic specific gravity of 0.401. These differences in densities partially explain why their moisture contents (in kilogram of water per cubic meter of dry wood) are slightly higher than ours at a given capillary pressure. Despite the fact that their values are systematically higher than the ones we found, the shape of the curves is similar.

Our measured values of the vapor diffusion resistance are lower than the previously published values, suggesting faster vapor transport, consistent with the faster liquid transport discussed above. For example, at 30% RH, the IEA Annex 14 lists μ values of red pine ranging from 200 to 500, and the Kumaran report lists a value of 490 (Kumaran *et al.* 2002, Hill *et al.* 2010). In contrast, all of our measurements were below 200. However, the differences between the literature values and those in this paper appear to decrease at higher relative humidity. At a mean of 70% RH, Kumaran reports a μ value of 40, which is with the range of values we measured for μ in the tangential direction at these relative humidities.

In short, the liquid water transport properties for both the untreated and ACQ-treated southern pine were much higher than the previously reported properties for pine. It is important to highlight that the lumber was partially colonized with a sap-stain (blue stain) fungus, and that these fungi are frequently thought to affect the wood-water relations (Findlay and Pettifor 1939, Schirp *et al.* 2003, Fojutowski 2004), although there is a lack of hard data on the type and magnitude of the modifications. Our data suggest that this colonization has a large effect on the liquid water transport properties. Sap-stain fungi selectively destroy bordered pits, and therefore explain the observed increased capillary absorption coefficients and lower water vapor diffusion factors. It is also interesting to note that the specimens that appeared to be further colonized with blue stain fungus also had higher maximum moisture content in the vacuum saturation experiments. However, there was no attempt to control or study the effect of blue stain in those measurements, so the trends in the maximum moisture content may be affected by observational bias. Our measurements suggest that the blue stain fungus greatly affects the interaction of liquid water with wood.

Conclusions

The hygric properties of untreated and ACQ-treated southern pine were collected with the goal of developing more accurate hygrothermal–corrosion models. The moisture storage was characterized by a combination of sorption isotherms and MIP and the moisture transport was characterized by water vapor diffusion cup tests and capillary absorption tests. The data were analyzed by combining the isotherm and porosimetry curve into a single

moisture retention curve. For the transport data, the diffusivity approach of Carmeliet was used to determine the moisture permeability over six orders of magnitude of capillary pressure.

The moisture storage and transport properties were similar between the untreated and ACQ-treated wood, except for the transport in the radial direction, which was slower for the ACQ-treated wood. It was hypothesized that the treatment process may affect the ray cells, which reduce transport. Values for the capillary absorption coefficient of both the treated and untreated wood were much higher than the previously published values, and this was attributed to the colonization by blue stain fungi.

Acknowledgments

Samuel L. Zelinka acknowledges funding from the Presidential Early Career Awards for Scientists and Engineers (PECASE). Research was funded by the Forest Products Laboratory of the US Forest Service.

Note

1. Personal communication with Dr Hannelore Derluyn, Ghent University.

References

Anon. (1936) *Southern Yellow Pine. Technical Note No. 214* (Madison, WI: US Forest Service Forest Products Laboratory).

Anon. (2007) *AWPA U1-06: Use Category System* (Granbury, TX: American Wood Preservers' Association).

Cao, J. and Kamdem, D. P. (2004) Moisture adsorption characteristics of copper-ethanolamine (Cu-EA) treated Southern yellow pine (Pinus spp.). *Holzforschung*, 58, 32–38.

Carmeliet, J., Janssen, H. and Derluyn, H. (2007) An improved moisture diffusivity model for porous building materials. *Proceedings of 12th Symposium for Building Physics* (Desden, Germany).

Carmeliet, J. and Roels, S. (2002) Determination of the moisture capacity of porous building materials. *Journal of Building Physics*, 25(3), 209–237.

Dennis, J. K., Zou, C. and Short, N. R. (1995) Corrosion behaviour of zinc and zinc alloy coated steel in preservative treated timber. *Transactions of the Institute of Metal Finishing*, 75, 96–101.

Dulat, J. (1980) The effects of borate preservatives and fire retardants on hygroscopicity and moisture content equilibria in timber. *Journal of the Institute of Wood Science*, 8, 214–220.

Durner, W. (1994) Hydraulic conductivity estimation for soils with heterogeneous pore structure. *Water Resources Research*, 30(2), 211–223.

Findlay, W. and Pettifor, C. (1939) The effect of sap-stain on the properties of timber III. Effect of sap-stain on the modulus of elasticity of scots pine sapwood. *Forestry*, 13, 146–147.

Fojutowski, A. (2004) The hygroscopicity and absorptiveness of blue-stained Scotch pine wood. *Annals of Warsaw Agricultural University. Forestry and Wood Technology*, 55, 216–221.

Glass, S. V., Zelinka, S. L. and Johnson, J. A. (2014) Investigation of historic equilibrium moisture content data from the Forest Products Laboratory. General Technical Report, FPL-GTR-229 (Madison, WI: Forest Service, Forest Products Laboratory).

Hens, H. (1991) *IEA Annex 14: Condensation and Energy, Vol. 3: Catalogue of Material Properties* (Paris: International Energy Agency).

Hill, C. A. S., Norton, A. and Newman, G. (2010) Analysis of the water vapour sorption behaviour of Sitka spruce [*Picea sitchensis (Bongard) Carr.*] based on the parallel exponential kinetics model. *Holzforschung*, 64, 469–473.

Holbrook, N. M., Zwieniecki, M. A. and Melcher, P. J. (2002) The dynamics of "dead wood": Maintenance of water transport through plant stems. *Integrative and Comparative Biology*, 42(3), 492–496.

Janssen, H., Blocken, B. and Carmeliet, J. (2007) Conservative modelling of the moisture and heat transfer in building components under atmospheric excitation. *International Journal of Heat and Mass Transfer*, 50(5–6), 1128–1140.

Kumaran, M. K., Lackey, J. C., Normandin, N., Tariku, F. and van Reenen, D. (2002) *A Thermal and Moisture Transport Property Database for Common Building and Insulation Materials. Final Report, ASHRAE Research Project RP-1018* (Atlanta, GA: American Society of Heating, Refrigerating and Air-Conditioning Engineers).

Lebow, S. (2004) Alternatives to chromated copper arsenate for residential construction. Research Paper, FPL-RP-618 (Madison, WI: Forest Service, Forest Products Laboratory)..

Lebow, S. (2010) Wood preservation. In R. J. Ross (ed.) *Wood Handbook – Wood as an Engineering Material* (Madison, WI: U.S. Department of Agriculture, Forest Service, Forest Products Laboratory), 508 p.

Neimsuwan, T., Wang, S., Taylor, A. M. and Rials, T. G. (2008) Statics and kinetics of water vapor sorption of small loblolly pine samples. *Wood Science and Technology*, 42(6), 493–506.

Schirp, A., Farrell, R. L., Kreber, B. and Singh, A. P. (2003) Advances in understanding the ability of sapstaining fungi to produce cell wall-degrading enzymes. *Wood and Fiber Science*, 35, 434–444.

Short, N. R. and Dennis, J. K. (1997) Corrosion resistance of zinc-alloy coated steel in construction industry environments. *Transactions of the Institute of Metal Finishing*, 75, 47–52.

Shupe, T. F., Lebow, S. T., Choong, E. T. and Xiong, M. (2001) Inadequate redrying linked to dimensional instability of CCA-treated southern pine lumber. *Forest Products Journal*, 51, 59–62.

Trenard, Y. (1980) Comparaison et Interpretation de Courbes Obtenues par Porosimétrie au Mercure sur Diverses Essences de Bois [Comparison and interpretation of curves obtained by mercury porosimetry on various wood species]. *Holzforschung*, 34(4), 139–146.

Vlosky, R. P. (2009) *Statistical Overview of the U.S. Wood Preserving Industry: 2007* (Vancouver, WA: North American Wood Pole Council).

Wiedenhoeft, A. C. (2010) Structure and function of wood. In R. J. Ross (ed.) *Wood Handbook – Wood as an Engineering Material* (Madison, WI: U.S. Department of Agriculture, Forest Service, Forest Products Laboratory), 508 p.

Zelinka, S. L., Derome, D. and Glass, S. V. (2010). From laboratory corrosion tests to a corrosion lifetime for wood fasteners: Progress and challenges. *Proceedings of the International Convention of Society of Wood Science and Technology and United Nations Economic Commission for Europe – Timber Committee* (Geneva, Switzerland: SWST, WS-96).

Zelinka, S. L., Derome, D. and Glass, S. V. (2011) Combining hygrothermal and corrosion models to predict corrosion of metal fasteners embedded in wood. *Building and Environment*, 46(10), 2060–2068.

Zelinka, S. L., Derome, D. and Glass, S. V. (2014) The effect of moisture content on the corrosion of fasteners embedded in wood subjected to alkaline copper quaternary treatment. *Corrosion Science*, 83, 67–74.

Zelinka, S. L. and Glass, S. V. (2010) Water vapor sorption isotherms for southern pine treated with several waterborne preservatives. *ASTM Journal of Testing and Evaluation*, 38, 80–88.

Zelinka, S. L. and Rammer, D. R. (2012) Modeling the effect of nail corrosion on the lateral strength of joints. *Forest Products Journal*, 62, 160–166.

Zelinka, S. L., Rammer, D. R. and Stone, D. S. (2008) Electrochemical corrosion testing of fasteners in extracts of treated wood. *Corrosion Science*, 50(5), 1251–1257.

Zelinka, S. L. and Stone, D. S. (2011) Corrosion of metals in wood: Comparing the results of a rapid test method with long-term exposure tests across six wood treatments. *Corrosion Science*, 53(5), 1708–1714.

Zhang, J. and Peralta, P. N. (1999). Moisture content-water potential characteristic curves for red oak and loblolly pine. *Wood and Fiber Science*, 31, 360–369.

Zillig, W. (2009). Moisture transport in wood using a multiscale approach (PhD thesis). (Leuven: Katholieke Universiteit Leuven).

Zillig, W., Janssen, H., Carmeliet, J. and Derome, D. (2006). Liquid water transport in wood: Towards a mesoscopic approach. In R. Ge and Desmarais (eds). *Research in Building Physics and Building Engineering* (London: Taylor & Francis), pp. 107–114.

Zwieniecki, M. A. and Holbrook, N. M. (2000) Bordered pit structure and vessel wall surface properties. Implications for embolism repair. *Plant Physiology*, 123(3), 1015–1020.